J. Fluid Mech. (1976), *vol.* 75, *part* 3, *pp.* 459–467
Printed in Great Britain

A boundary-layer model of flow in a porous medium at high Rayleigh number

By J. L. ROBINSON
Applied Mathematics Division, DSIR, Wellington, New Zealand

AND M. J. O'SULLIVAN
Department of Theoretical and Applied Mechanics, University of Auckland, New Zealand

(Received 24 June 1975 and in revised form 19 January 1976)

A boundary-layer model, based on computational results, describes a number of features of two-dimensional convection in a porous medium: the heat flux, velocity, length and temperature scales and the pattern of flow. The cell structure is different from that for convection in a viscous fluid. The model is valid for a limited range of the Rayleigh number.

1. Introduction

Two-dimensional boundary-layer models provide useful aids in the description of fluid flows at high values of the Rayleigh number, both in predicting the dependence of the heat flux, velocities, length scales and temperatures on the Rayleigh number, and in describing qualitative flow features. For example Robinson (1967) has treated steady cellular flow in fluids with Prandtl numbers of order unity for the cases of all boundaries rigid, rigid horizontal and free vertical boundaries (stress-free), and all boundaries free, Turcotte & Oxburgh (1967) have described certain features of convection in the earth's mantle using an infinite Prandtl number model with all boundaries free, and Robinson (1973) has based a discussion of the development of fluctuations in thermal convection on a boundary-layer model.

There are significant differences between the flow of a fluid in a porous medium and the motion of a viscous fluid: for example, there is no diffusion of vorticity in a porous medium. Therefore it is necessary to develop a new boundary-layer model to describe the fluid behaviour in a porous medium.

Whereas the boundary-layer models for flow in a viscous fluid all include a moving isothermal interior region, in a porous medium the ascending and descending plumes, which are boundary layers in the model, occupy the entire space away from the boundary layers on the horizontal plates. Since with the relaxation of constraints implied by these flow features the system of model balances is no longer fully determined, the boundary-layer analysis is based on two results from computations.

In this way a boundary-layer model has been developed which fits the remaining computational data, and describes the qualitative features of the flow. The $\frac{4}{3}$-power law dependence of Nusselt number on Rayleigh number suggested here provides a good fit to the band of experimental points available.

2. Equations

The field variables can be conveniently made dimensionless by choosing as units of length, temperature, pressure and velocity

$$H, \quad \tfrac{1}{2}\Delta T, \quad \rho_0 \nu\kappa/k, \quad \kappa/H,$$

where H is the plate separation, ΔT is the temperature difference between the plates, ρ_0 is the density of the fluid at the mean temperature, ν is the kinematic viscosity of the fluid, κ is the thermal diffusivity and k is the permeability.

For steady two-dimensional motion the field equations, simplified by the Boussinesq approximation, can be written with the above units in dimensionless form (Wooding 1956):

$$u = -\partial p/\partial x, \tag{1}$$

$$v = -\partial p/\partial y + \tfrac{1}{2}AT, \tag{2}$$

$$u\frac{\partial T}{\partial x} + v\frac{\partial T}{\partial y} = \frac{\partial^2 T}{\partial x^2} + \frac{\partial^2 T}{dy^2}. \tag{3}$$

The dimensionless parameter of the flow is the Rayleigh number

$$A = g\alpha\Delta T k H/\kappa\nu,$$

where g is the gravitational acceleration and α is the coefficient of thermal expansion of the fluid. The flow region considered is a closed rectangular box (figure 1) with thermally insulated walls and non-dimensional temperatures of $T = 1$ at the base and $T = -1$ at the top.

The computations were carried out to determine the horizontal cell width which maximized the heat flux at a number of values of the Rayleigh number, and the values of other flow variables as well as the flow configuration were determined. These calculations were carried out assuming that the flow is two-dimensional and steady. Other computations (Horne & O'Sullivan 1974) suggest that the flow may be unsteady at higher Rayleigh number and experimental work indicates that the preferred mode of convection may be three-dimensional and unsteady (Caltagirone, Cloupeau & Combarnous 1971). However, the experimental results of Elder (1967) in the constrained two-dimensional configuration of a Hele Shaw cell do confirm the existence of cells such as those computed here.

3. Boundary-layer analysis

Past attempts to develop a boundary-layer model of convection in a porous medium include the consideration of the horizontal boundary layer alone by Elder (1967), which suggested the linear dependence of Nusselt number on

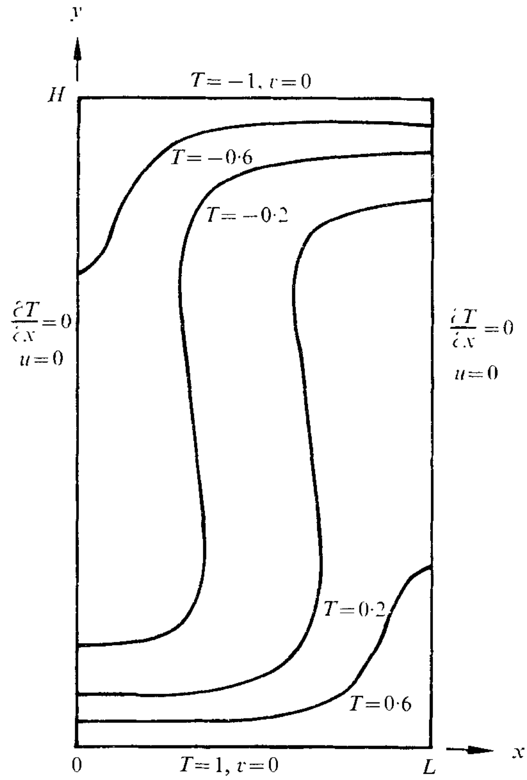

FIGURE 1. Flow region and boundary conditions.

Rayleigh number found for a limited range of Rayleigh number in some experiments, but which implied a zero vorticity in the horizontal boundary layer. This analysis cannot be extended to a complete cell (Robinson 1969) since the matching of the zero vorticity in the boundary layer on to the interior solution leads to the contradiction that the boundary-layer thickness is not small.

Palm, Weber & Kvernvold (1972) described a zero-velocity isothermal interior, and assumed a temperature of order unity in the vertical boundary layers. They derived a Nusselt number, Rayleigh number dependence of $Nu \sim A^{\frac{1}{2}}$. Again the analysis of Robinson suggests that this model will not be fully self-consistent. This may be seen as follows. In the model of Palm *et al.* the horizontal velocity in the horizontal boundary layers (which are of thickness of order $A^{-\frac{1}{2}}$) is of order A. The leading term in the vorticity equation in those boundary layers (obtained by taking the curl of the vector momentum equation) is then $\partial u/\partial y$, of order $A^{\frac{3}{2}}$. If this is matched to the zero-velocity interior it follows that the horizontal velocity is zero to this order within these boundary layers and the analysis thus breaks down.

The following alternative argument against the existence of an interior region in a steady-state solution illustrates the qualitative difference between the flow pattern in a porous medium and in a viscous fluid.

In a viscous fluid the interior region is moving (Pillow 1952; Turcotte &

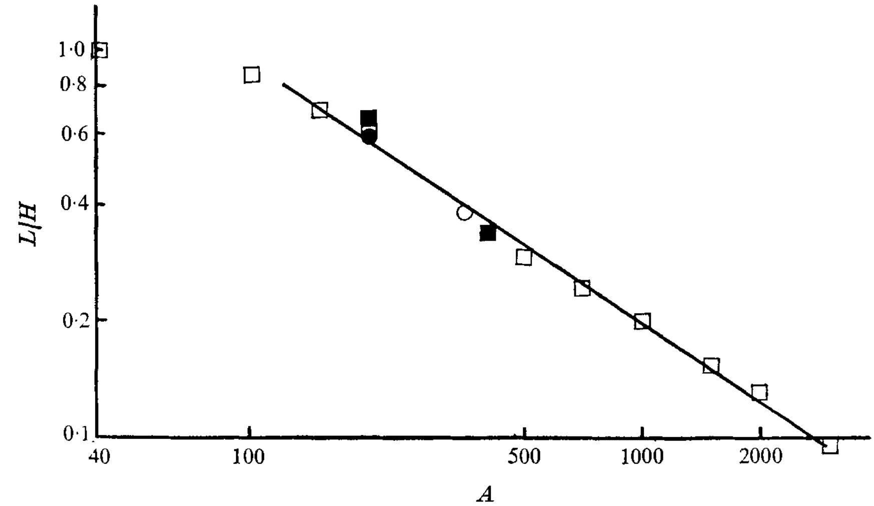

FIGURE 2. Aspect ratio of the cell L/H as a function of Rayleigh number A. The best-fit curve $L/H = 1{\cdot}7(A/A_c)^{-\frac{2}{3}}$ is shown together with computed results. □, O'Sullivan; ■, Combarnous (1970); ○, Combarnous & Bia (1971); ●, Vlasuk (1972).

Oxburgh 1967; Robinson 1967, 1969). A fluid particle at the outer edge of this interior region then alternately passes hot and cold boundary-layer regions, and the constant-temperature interior region is maintained.

In a porous medium the interior region would be at rest (Palm *et al.* 1972). A fluid particle at the outer edge of such a motionless interior region will then remain adjacent to a boundary layer having a temperature which is fixed in time and would thus tend towards that temperature. The buoyancy force would then accelerate the particle, which would join in the motion of the boundary layer. In this manner the boundary layer will entrain fluid from the interior until the interior region is destroyed. Thus an interior region will not be a feature of a steady-state solution for convection in a porous medium.

A boundary-layer model can only be constructed for flow in a porous medium provided that (*a*) there is no interior region, i.e. the vertical boundary layers occupy the entire cell, which has a horizontal length scale dependent on the Rayleigh number, and (*b*) not all of the mass circulation passes through the horizontal boundary layers; and indeed these flow features are evident in the computed results. The temperatures in the vertical boundary layers must then also be dependent on the Rayleigh number. With the relaxation of constraints implied by these flow features, the system of balances is no longer fully determined. The boundary-layer analysis is therefore based on two results from computations: that the horizontal cell width L for maximum heat flux varies as $L/H \sim A^{-\frac{2}{3}}$ and that the Nusselt number varies as $Nu \sim A^{\frac{2}{3}}$. Figures 2 and 3 illustrate this dependence. The best-fit curves are

$$Nu = 1{\cdot}55(A/A_c)^{\frac{2}{3}}, \quad L/H = 1{\cdot}7(A/A_c)^{-\frac{2}{3}}, \qquad (4), (5)$$

where $A_c = 4\pi^2$ is the critical Rayleigh number.

In the vertical boundary layers the flow is driven by the buoyancy force,

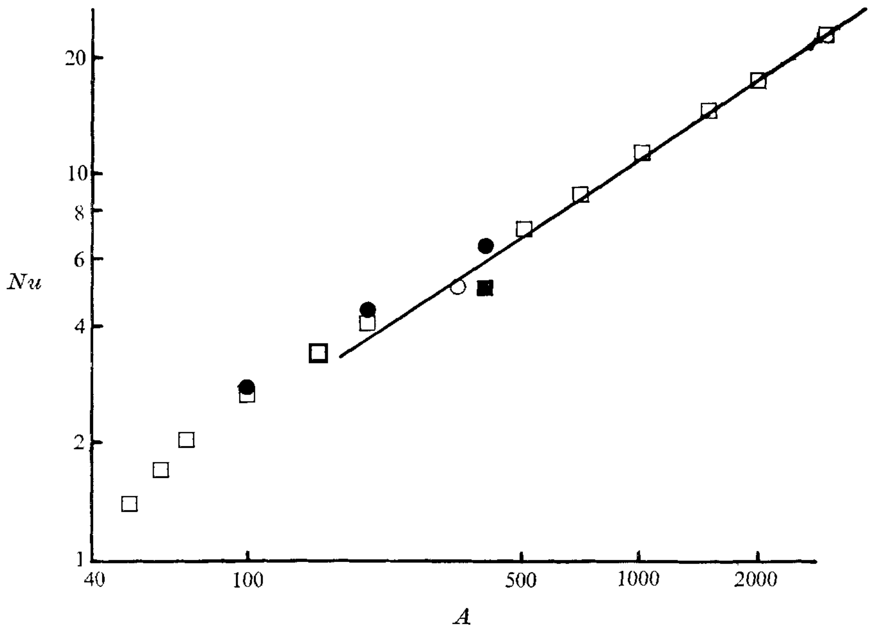

FIGURE 3. Nusselt number Nu *vs.* Rayleigh number A. The best-fit curve $Nu = 1{\cdot}55(A/A_c)^{\frac{2}{3}}$ is shown. The computed results are from the sources noted in figure 2.

$v \sim AT$, and the heat flux, vT, per unit horizontal length is proportional to $A^{\frac{2}{3}}$. Dependences of $v \sim A^{\frac{5}{6}}$ and $T \sim A^{-\frac{1}{6}}$ are predicted in this region. Figures 4 and 5 illustrate these dependences, and it is seen that the agreement with the computed results is excellent. The best-fit curves are

$$v(L, \tfrac{1}{2}H) = 11(A/A_c)^{\frac{5}{6}}, \quad T(L, \tfrac{1}{2}H) = 0{\cdot}5(A/A_c)^{-\frac{1}{6}}. \qquad (6), (7)$$

In the horizontal boundary layers, the boundary-layer width will be the inverse of the Nusselt number, and there must be a balance between the heat conduction and convection. Thus $u \sim (L/H)Nu^2$ in those regions. A dependence of $u \sim A^{\frac{2}{3}}$ is predicted. Figure 4 illustrates this dependence, and it is seen that the agreement with the computed results is again excellent. The best-fit curve is

$$u(\tfrac{1}{2}L, 0) = 11(A/A_c)^{\frac{2}{3}}. \qquad (8)$$

For each cell the dimensionless mass flux in the vertical boundary layers is of order $A^{\frac{1}{6}}$, and the dimensionless mass flux in the horizontal boundary layers is of order unity. Thus there is a greater mass flux in the vertical boundary layers than in the horizontal boundary layers, and not all of the mass flux passes through the horizontal boundary layers. This flow feature is reflected in the magnitude of the temperature in the vertical boundary layers: $T \sim A^{-\frac{1}{6}}$. This qualitative behaviour is found in the computed results, as illustrated in figure 6, where for a Rayleigh number of 1000, the flow between the streamlines $\psi = 0{\cdot}6\,\psi_{max}$ and $\psi = \psi_{max}$ joins the boundary layer after it has left the horizontal boundaries, and there is a rapid spreading of the hot plume in this region together with a rapid decrease in the temperature of the plume.

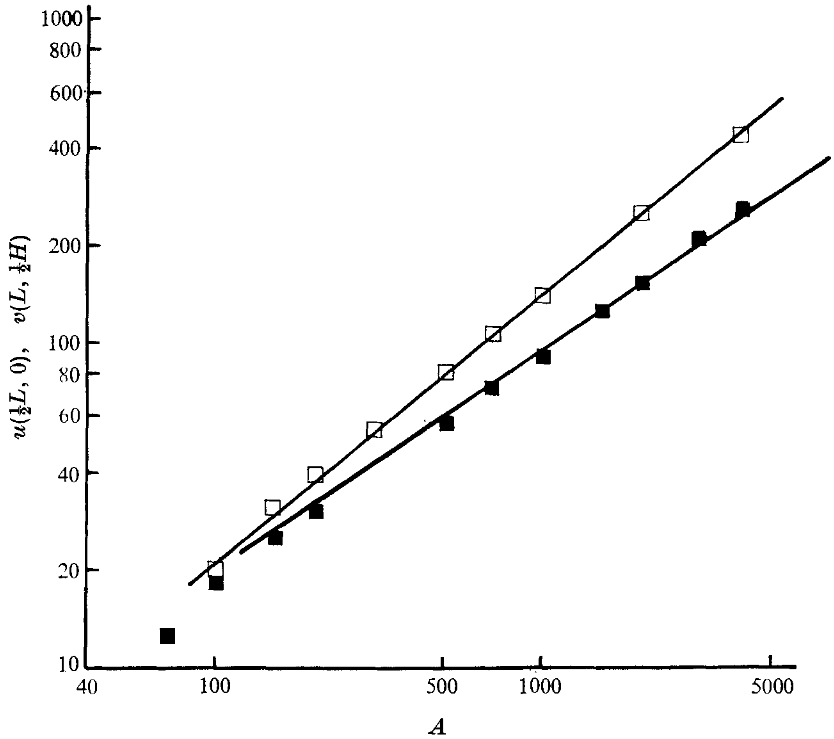

FIGURE 4. Computed values of $v(L, \frac{1}{2}H)$ and $u(\frac{1}{2}L, 0)$ together with best-fit curves. □, $v(Lm\ \frac{1}{2}H)$; ■, $u(\frac{1}{2}L, 0)$.

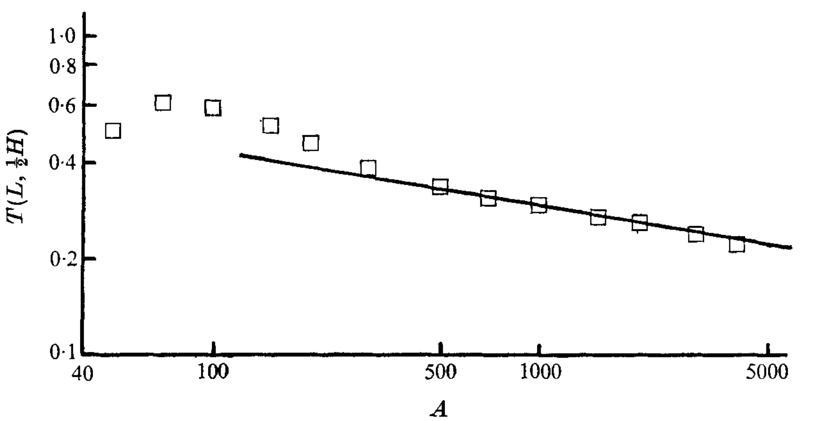

FIGURE 5. Computed values of $T(L, \frac{1}{2}H)$ together with the best-fit curve $T(L, \frac{1}{2}H) = 0{\cdot}5\,(A/A_c)^{-\frac{1}{6}}$.

The model suggests that in the vertical boundary layers the heat convection term $v\,\partial T/\partial y$ is of order of magnitude $A^{\frac{5}{6}}$ and the conduction term $\partial^2 T/\partial x^2$ is of order of magnitude $A^{\frac{7}{6}}$. This modelling remains valid so long as the conduction term does not dominate, for in that case the heat flux will diffuse from the rising plume into the descending plume, the interior temperature gradients (away from the horizontal boundaries) will decrease, and the flow will move more slowly.

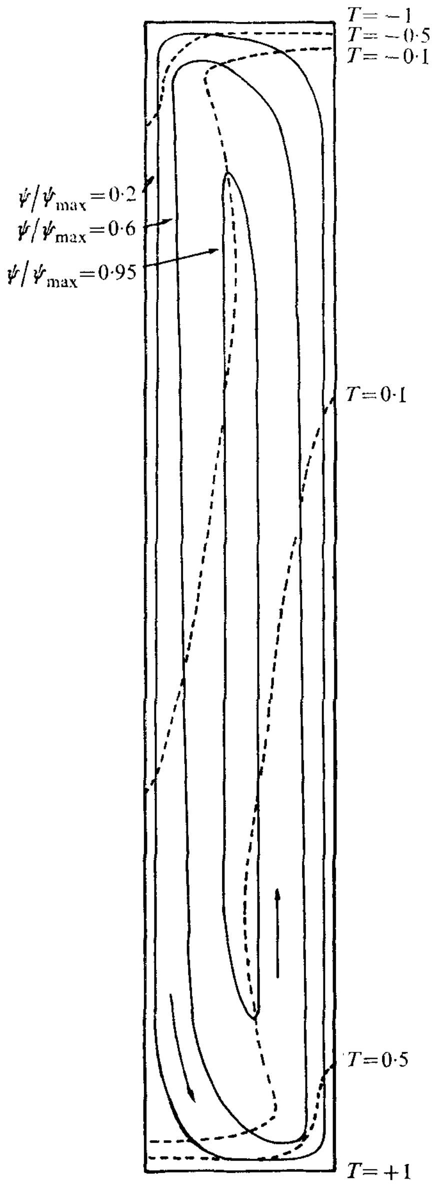

FIGURE 6. Temperature and stream-function contours. $A = 500$. $\psi_{\max}$ = maximum value of the stream function.

It is thus evident that the model will not be valid for sufficiently large values of the Rayleigh number. An estimate of the maximum Rayleigh number for which the model description may be expected to hold is obtained by equating the estimates for the vertical velocity v and the diffusion factor $(L/H)^{-2}$. The required balance is

$$v \simeq (L/H)^{-2}, \tag*{9)}$$

i.e.

$$11(A/A_c)^{\frac{5}{6}} \simeq (A/A_c)^{\frac{4}{3}}/2{\cdot}9, \tag{10}$$

i.e.

$$A \simeq 1000\,A_c. \tag{11}$$

In the range considered here, $A_c < A < 1000A_c$, the convection term will dominate, and the model provides a valid description. For Rayleigh numbers greater than about $1000A_c$ the model fails, and the flow will not follow this pattern.

Robinson (1973) has similarly developed a boundary-layer model for convection in a viscous fluid bounded by rigid horizontal boundaries, which was valid for a restricted range of the parameters. In that case an energy balance could be satisfied for some range of the Rayleigh number and the failure of the modelling provided a description of the development of a fluctuating motion.

It is also necessary to check the predicted magnitudes of the pressure variations, as earlier modelling attempts did not achieve self-consistency. From (1), (5) and (8) the pressure difference along the horizontal boundary layers is of order unity. From (2) and (6) the pressure difference along the vertical boundary layers is of order $A^{\frac{5}{6}}$ *or smaller*. Self-consistency is obtained by the requirement that the first-order vertical velocity equation is

$$v = \tfrac{1}{2}AT, \qquad (12)$$

and the horizontal pressure differences are balanced by lower-order terms.

It is worth noting that, by scaling the Rayleigh number by its critical value $A_c = 4\pi^2$, the constants in the best-fit curves for the temperature, Nusselt number and length scales are all of order unity; note (4), (5), (9) and (11). The values of the constants for the velocities are larger. This is self-consistent: (7) and (12) combine to give $v(L, \tfrac{1}{2}H) = 10(A/A_c)^{\frac{5}{6}}$, close to the value noted in (6).

4. Relevance of the model

The above analysis has limited practical significance since the steady two-dimensional flow considered may not be the preferred mode in a porous medium. The experiments of Elder (1967) show that two-dimensional cells of the type considered here do occur in the analogous Hele Shaw cell experiments. However, even these experiments show that the flow may not be steady. This is confirmed by the recent computations by Horne & O'Sullivan (1974), which indicate that alternative two-dimensional regimes may be possible, one being steady and including a number of narrow cells similar to those described here, the other unsteady and with horizontal length scales of the order of the plate separation. The heat flux is however similar in the two regimes.

The $\frac{2}{3}$-power law dependence of the Nusselt number on the Rayleigh number suggested here provides a good fit to the majority of the experimental data (figure 7). The linear dependence indicated by some experimental results (Elder 1967) and by both a simple dimensional argument and an upper-bound estimate (Gupta & Joseph 1973) lies above most of the experimental data. Some experimental data (Schneider 1963; Combarnous 1970) have shown further that the mean heat transfer does not depend solely on the Rayleigh number but also on the thermal characteristics of the constituting phases: the solid matrix and the saturating fluid. Thus for large Rayleigh numbers the basic assumptions of (1) and (2) may be invalid. Further experiments, with a more careful choice of

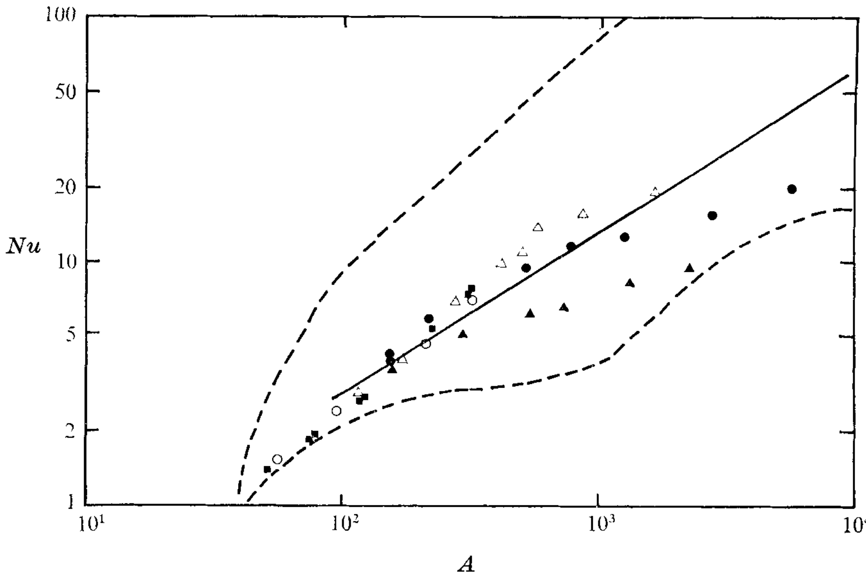

FIGURE 7. Comparison of experimental results and the theoretical curve for Nusselt number *Nu vs.* Rayleigh number *A*. ——, theoretical curve; ■, ●, □, ○, experimental points (see Palm *et al.*); – – – –, bounds for experimental data (see Busse & Joseph 1972).

grain size, need to be conducted before theoretical and experimental results can be satisfactorily compared.

Although the model developed here adequately describes two-dimensional steady motion in a porous medium, the problem of the three-dimensional or transient character and the non-uniqueness of the flow remains unexplained.

REFERENCES

BUSSE, F. H. & JOSEPH, D. D. 1972 *J. Fluid Mech.* **54**, 521.

CALTAGIRONE, J. P., CLOUPEAU, M. & COMBARNOUS, M. A. 1971 *Comptes Rendus Acad. Sci. Paris*, B **273**, 833.

COMBARNOUS, M. A. 1970 *Rev. Gén. Thermique*, **9**, 1377.

COMBARNOUS, M. A. & BIA, P. 1971 *Soc. Pet. Engrs J.* **4**, 399.

ELDER, J. W. 1967 *J. Fluid Mech.* **27**, 29.

GUPTA, V. P & JOSEPH, D. D. 1973 *J. Fluid Mech.* **57**, 491.

HORNE, R. N. & O'SULLIVAN, M. J. 1974 *J. Fluid Mech.* **66**, 399.

PALM, E., WEBER, J. E. & KVERNVOLD, O. 1972 *J. Fluid Mech.* **54**, 153.

PILLOW, A. F. 1952 *Astr. Dept. Supply Aero. Res. Lab. Rep.* A79.

ROBINSON, J. L. 1967 *J. Fluid Mech.* **30**, 577.

ROBINSON, J. L. 1969 *Int. J. Heat Mass Transfer*, **12**, 1257.

ROBINSON, J. L. 1973 *N.Z. J. Sci.* **16**, 389.

SCHNEIDER, K. J. 1963 *11th Cong. Refrigeration (Munich)*, paper 11–4.

TURCOTTE, D. L. & OXBURGH, E. R. 1967 *J. Fluid Mech.* **28**, 29.

VLASUK, M. P. 1972 *Minsk. Paper*, no. 1–49 (trans. from Russian into French by M. A. Combarnous, private communication).

WOODING, R. A. 1956 *J. Fluid Mech.* **2**, 273.